Progress In Electromagnetics Research C, Vol. 121, 39–48, 2022

UWB Monopole Antenna with Dual Notched Bands Verified by Characteristic Mode Analysis (CMA)

Subrahmanyam Grandhi Venkata[1, *] and Sri Rama Krishna Kalva[2]

Abstract—An ultra-wideband (UWB) antenna with dual band notched characteristics verified by characteristic mode analysis (CMA) is presented. The intended UWB radiator is etched on a Rogers RT5880 substrate with a size of $29 \times 35 \times 0.764\,\text{mm}^3$, operating over a spectrum of 2.66–14.86 GHz with a fractional bandwidth (FBW) of 139%. Dual notched bands at WiMAX (3.01–3.63 GHz) and WLAN (4.48–5.85 GHz) are achieved by embedding L-shaped stubs in the notched rectangular patch. In addition, the two notched bands of the reported antenna are verified by using characteristic mode analysis (CMA) in terms of modal significance (MS) and characteristic angle (CA). The reported antenna's simulated and tested results are well matched to obtain S_{11}, VSWR, stable radiation patterns, a stable peak gain of 2.65 to 3.6 dBi, and the maximum radiation efficiency of 97.86% in frequency domain, which make the intended radiator suitable for portable UWB applications.

1. INTRODUCTION

Due to the need for handling more people and more data, wideband wireless technology is in high demand these days. For commercial usage, the US Federal Communications Commission (FCC) authorised a frequency range with a bandwidth of 3.1–10.6 GHz in 2002, which has gained significant interest from academia and industry [1]. Then onwards, the use of UWB technology has become one of the most extensively used technologies in advanced wireless communication due to short range and high data rate with low energy level. The development of UWB antenna is also playing a crucial role in UWB communication because designing a wide impedance bandwidth over a UWB function is one of the important properties of UWB communication systems. Thus, to meet this wide-band function, several researchers have proposed a variety of antenna structures. However, over the designated UWB frequency, it may cause interference due to existing narrow-bands, such as WiMAX and WLAN [2, 3]. To overcome this interference problem, the UWB antennas with band-notch characteristics are desirable. For achieving notch characteristics with UWB elements, several techniques have been reported in the literature [4–10]. The commonly used methods are based on etching slots on the radiating surface and/or in the ground plane [4–7], adding a parasitic element(s) near the radiating element, etc. [8–10]. Usually, one slot/parasitic element is sufficient to generate a single-notch [11]. However, to generate dual-notches requires either two different slots or two parasitic elements with different lengths. Further, the notch-frequency generated using slots or parasitic elements cannot be adjusted after fabrication.

To comprehend the band notch performance in more depth, it is required to analyse the radiators with their lumped equivalent circuits, which is not reported in above literature. Moreover, the proposed work is also focused on analysing the lumped equivalent circuit of notched elements of the proposed antenna, but the behavior of quadruple notched elements can be better understood with characteristic mode analysis (CMA). Several investigations have shown that characteristic mode analysis (CMA) can

Received 11 May 2022, Accepted 30 May 2022, Scheduled 23 June 2022

* Corresponding author: Subrahmanyam Grandhi Venkata (subrahmanyam.grandhi@gmail.com).

[1] Department of ECE, College of Engineering and Technology, Acharya Nagarjuna University, Guntur, India. [2] Potti Sriramulu Chalavadi Mallikarjuna Rao, College of Engineering and Technology, Vijayawada, India.

provide an in-depth physical knowledge of the antenna's working mechanism [12]. It exhibits inherent electromagnetic resonance parameters such as current distribution and far-field radiation pattern [13]. These statistics might well be used to assess the antenna's performance as well as aid in the optimization process [14–16]. In 1971, Garbacz et al. introduced a novel theory called "Characteristic Mode Analysis" (CMA) [17]. The number of modes usually depends on conducting material size. Equation (1) [12] depicts the inherent relationship between modal currents and the modal impedance matrix.

$$X\left(J_n\right) = \lambda_n R\left(J_n\right) \tag{1}$$

where J_n represents "the modal currents", and λ_n represents "the eigen values". The range of λ_n is $-\infty$ to $+\infty$, and the resonant values occur when λ_n is zero. The modal significance (MS) is the parameter used to identify the resonant frequencies of conducting material, and it is related to the eigen vector. The relation between MS and λ_n is represented in Equation (2) [15]. The characteristic angle (CA) is another important part that helps figure out how conductive planes behave electrically. The relation between CA and λ_n is shown in Equation (3) [12].

$$\text{MS} = \left|\frac{1}{1+j\lambda_n}\right| \tag{2}$$

$$\text{CA} = 180^\circ - \tan^{-1}\left(\lambda_n\right) \tag{3}$$

The CMA theory might aid in understanding the electrical behavior of materials by analyzing surface current distributions. Modes are the orthogonal currents that flow in the conducting planes. Following the cited literature, very simple dual notched-bands with independent control of notch frequency design is proposed in this paper.

The designed antenna prototype is fabricated on a Rogers RT5880 substrate with a size of $29 \times 35 \times 0.764\,\text{mm}^3$ and validates the simulated results. The other advantage of the proposed approach is to avoid the interference of both WiMAX and WLAN frequency bands independently. The designed antenna operates in 2.66–14.86 GHz frequency range. The work is organized as follows. In Section 2, the optimized design of proposed antenna is discussed. In Section 3, step by step design procedures of the reported antenna, parametric study of notched bands, and CMA analysis of notched bands are discussed. Section 4 presents the conceptual antenna's frequency domain simulated and measured results. Section 5 provides the conclusion of the proposed work.

2. ANTENNA DESIGN

The proposed radiator is printed on a Rogers RT5880 substrate with a size of $W_S \times L_S$ and thickness of 0.764 mm along with a microstrip line feed of $W_F \times L_F$ as depicted in Figure 1(a). The proposed antenna consisting of notched rectangular bevels of $g \times h$ at the lower edge of a rectangular patch structure of $a \times i$ etched on top of the substrate along with a rectangular defected ground structure (RDGS) of dimension $W_S \times L_G$ is printed below the substrate to achieve UWB bandwidth [18]. To realize the two notched bands, the proposed UWB antenna and L-type stubs are on top and sides of the patch structure with dimensions of $b \times c$ and $d \times e$, respectively. The optimized dimensions of the proposed antenna are: $W_S = 29\,\text{mm}$, $L_S = 35\,\text{mm}$, $W_F = 2.5\,\text{mm}$, $L_F = 14.5\,\text{mm}$, $L_G = 14\,\text{mm}$, $a = 17$, $i = 15$, $b = 2\,\text{mm}$, $c = 1.3\,\text{mm}$, $d = 2\,\text{mm}$, $e = 10.8\,\text{mm}$, $f = 0.3\,\text{mm}$, $g = 3\,\text{mm}$, $h = 3\,\text{mm}$. The prototype of the proposed antenna is shown in Figure 2.

3. PARAMETRIC STUDY OF PROPOSED ANTENNA

In this section, the parametric study of the reported UWB antenna with varying ground and patch structures is discussed in Section 3.1. The parametric analysis of L-type notched band elements to reject WiMAX and WLAN bands is discussed in Section 3.2. In Section 3.3, the notched bands of the intended radiator are verified by characteristic mode analysis.

3.1. Basic UWB Antenna with Varying Patch and Ground

The step-by-step design process of the basic UWB antenna is depicted in Figures 3(a)–(c), and their S_{11} parameter plot is depicted in Figure 4. The antenna structure, Ant#1, consisting of a rectangular patch

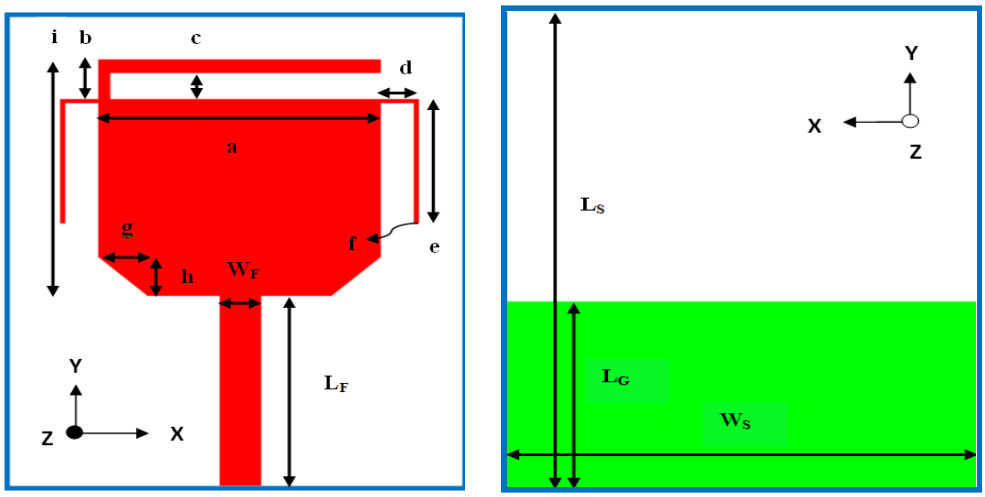

Figure 1. Geometry of proposed antenna. (a) Top view and (b) bottom view.

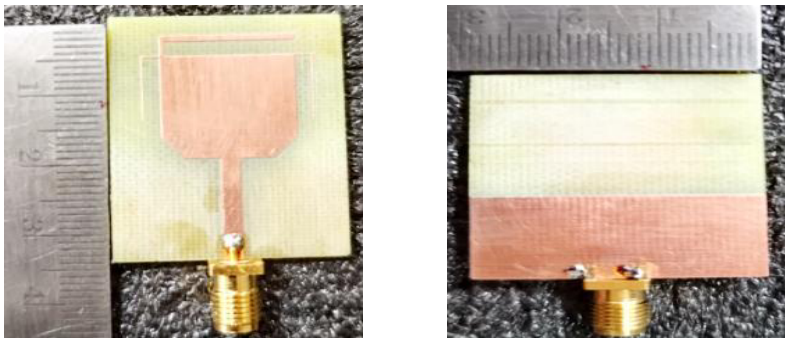

Figure 2. Prototype of the proposed antenna. (a) Top view and (b) bottom view.

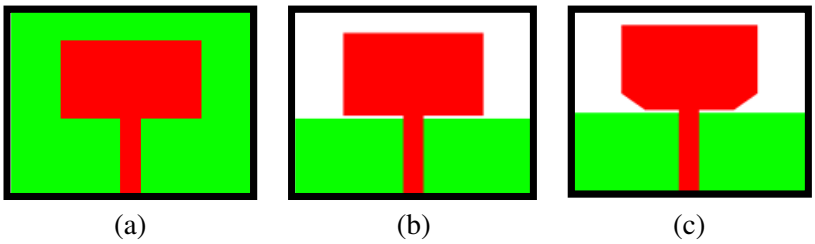

Figure 3. Evolution of basic UWB radiator. (a) Ant#1, (b) Ant#2, (c) Ant#3.

structure is embedded with a 50 Ω microstrip line along with a full ground plane as shown in Figure 3(a). From Figure 4, it is noticed that the antenna structure Ant#1 does not produce any resonances within the operating UWB bandwidth. To improve the impedance matching [19], the structure Ant#1 is etched with a rectangular defective ground structure to obtain Ant#2 as depicted in Figure 3(b). An impedance bandwidth of 4.72 GHz with a spectrum covering 3.52–8.24 GHz, with a peak value of S_{11}, is −20.9 dB at 4.32 GHz which is noticed from Figure 4, for the antenna structure Ant#4. The antenna structure Ant#3 is obtained by etching bevels at the lower end of the antenna structure [20] and Ant#2

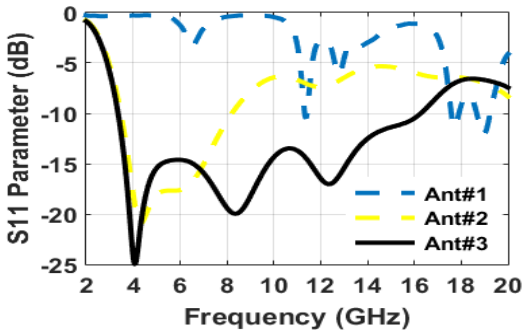

Figure 4. S_{11} plot of basic UWB radiator.

to obtain the bandwidth of the proposed UWB element ranging from 3.3–16.31 GHz with FBW of 133% as depicted in Figure 4.

3.2. UWB Antenna with WiMAX and WLAN Band Rejection

To obtain notched bands at WiMAX and WLAN, L-type stubs are etched on top of the patch and on both sides of the patch structure, respectively to achieve notch centre frequencies at 3.42 GHz and 5.31 GHz, respectively. Here, L-type stubs operate as quarter-wavelength resonators and the centre of notched frequencies f_{ni} of two notched bands are approximated by [21],

$$f_{ni} = \frac{C}{4\sqrt{\frac{\epsilon_r + 1}{2}} L_{Ti}} \tag{4}$$

where C is the velocity of light, L_{Ti} the total length of the L-type stubs, and $i = 1, 2$. According to Equation (1), when the total length, L_{T1}, of the upper L-type stub is varied in steps of 17 mm, 19 mm ($p*$), and 21 mm, the notch centre frequencies are achieved at 3.67 GHz, 3.42 GHz, and 3.24 GHz with a span of bandwidths ranging from 3.31–4.08 GHz, 3.04–3.89 GHz, and 2.83–3.79 GHz, respectively to notch WiMAX band as shown in Figure 5(a). To notch the WLAN band, an L-type stub is etched on both sides of the patch structure which is utilized with total length L_{T2}. When L_{T2} is changed in steps of 10.8 mm, 12.8 mm ($P*$), and 14.8 mm, the bandwidths of the proposed antenna are achieved in between 4.86–6.75 GHz, 4.37–5.85 GHz, and 3.95–5.28 GHz with centre of notch bands at 6.17 GHz, 5.31 GHz, and 4.62 GHz, respectively as depicted in Figure 5(b). The parametric analysis of notched bands of the proposed antenna is depicted in Table 1.

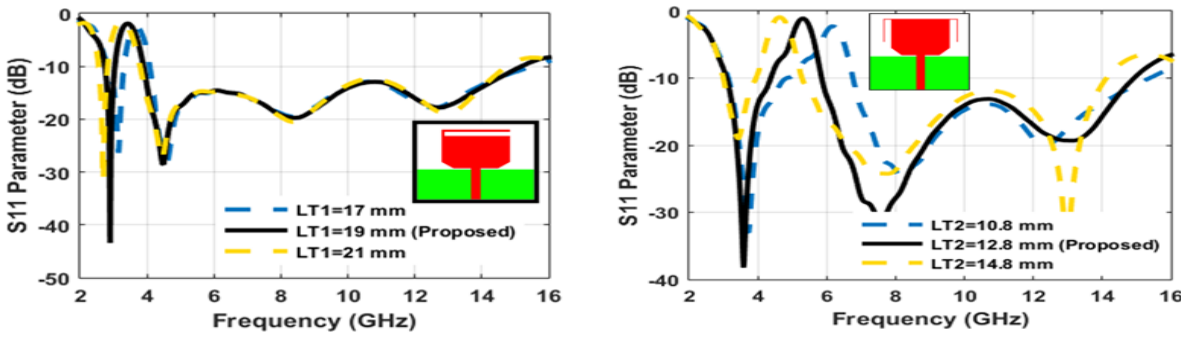

Figure 5. S_{11} plot of proposed UWB antenna with WiMAX and WLAN notched bands with varying stub lengths, L_{T1} and L_{T2}. (a) WiMAX band notch, (b) WLAN band notch.

Table 1. Parametric analysis of notched elements of reported antenna.

Notched element	Stub length, L_{Ti} (mm)		Magnitude of length error, %	Notch centre frequency, f_n (GHz)	Defined Bandwidth, (GHz)	Obtained Bandwidth, (GHz)
	Simulated	Calculated				
Stub, S_1	17	19.0	10.5	3.67	3.3–3.6 (WiMAX)	3.31–4.08
	19 (P*)	**20.4**	**6.8**	**3.42**		**3.04–3.89**
	21	21.63	2.9	3.24		2.83–3.79
Stub, S_2	10.8	11.3	4.4	6.17	3.7–4.2 (C-band)	4.86–6.75
	12.8 (P*)	**13.1**	**2.2**	**5.31**		**4.37–5.85**
	14.8	15.17	2.4	4.62		3.95–5.28

P* — Proposed

3.3. Notch Behavior of Proposed EEP-UWB Antenna Checked with Characteristic Mode Analysis (CMA)

The dual band notched characteristics of proposed radiator are verified by theory of characteristic mode analysis in terms of modal significance and characteristic angle.

Figures 6(a) and (b) depict the representation of MS and CA responses of the intended dual band notched radiator with 7 modes. The plots shown in Figures 6(c)–(f) clearly indicate that two notched bands are achieved with the characteristics of MS and CA. From Figures 6(c) and (d), it is noticed that the WiMAX band is notched at mode 2, and from Figures 6(e) and (f), the WLAN band is notched at mode 6. All these MS and CA are well matched with the S-parameter results of the proposed radiator.

4. RESULTS AND DISCUSSION

The intended dual band notched UWB antenna performance was analysed by simulation with commercialized software CST Microwave Studio ver.2021. An Anritsu MS2037C/2 network analyzer was used to test the proposed antenna's electrical properties. The frequency domain features such as S_{11}, VSWR, peak gain, radiation efficiency, patterns, and surface current distributions of the suggested dual notched radiator are evaluated. Figures 7(a), (b) show the results of S_{11} simulations and measurements, as well as VSWR plots for the suggested antenna. From Figure 7(a), it can be seen that the suggested antenna has a 139% impedance bandwidth, which covers the whole UWB from 2.66 to 14.86 GHz except for two notched bands having centre frequencies of 3.3 and 5.33 GHz with notched bandwidths of 617 MHz and 1374 MHz, respectively. Figure 7(b) shows the simulated and measured VSWR plots with VSWR values of 7.02 and 16.35 being noticed at notch centre frequencies of 3.3 and 5.33 GHz, respectively. The minor discrepancies between simulated and measured results may be owing to manufacturing and measurement flaws, the SMA interconnection, or parametric discrepancies between measured and simulated parameters.

The measured peak gain for the reported radiator is depicted Figure 7(c). It is observed from Figure 7(c) that the peak gain of basic UWB element varies between 2.65 and 3.6 dBi with an average gain of 3.54 dBi over the operating UWB. For the intended dual band notched UWB radiator, the gain fluctuates from 2.94 dBi to 4.82 dBi with an average gain of 3.07 dBi and abruptly falls to -5.23 dBi and -8.25 dBi at notch frequencies of 3.3 and 5.33 GHz, respectively. The abrupt change of gain at 3.3 GHz and 5.33 GHz confirms that the proposed antenna effectively eliminates the interference [22] due to WiMAX and WLAN bands, respectively. Similarly, the abrupt changes in radiation efficiencies of 40.23% and 28.23% are noticed at 3.3 GHz and 5.33 GHz to notch WiMAX and WLAN bands, respectively, as shown in Figure 7(d). The peak value of radiation efficiency of reported element is noticed to be 97.85% at 8.3 GHz. Figure 7(e) shows the simulated and measured 2-dimensional patterns of the intended radiator at 2.88 and 3.89 GHz. Figure 7(e) shows that the radiation patterns of the recommended antenna are approximately omnidirectional in the H-plane and monopole-like in the E-plane. At higher frequencies, the amplitude of higher order modes increases, and the phase of the waves is not evenly distributed across the antenna's aperture. This results in a distorted radiation pattern [23].

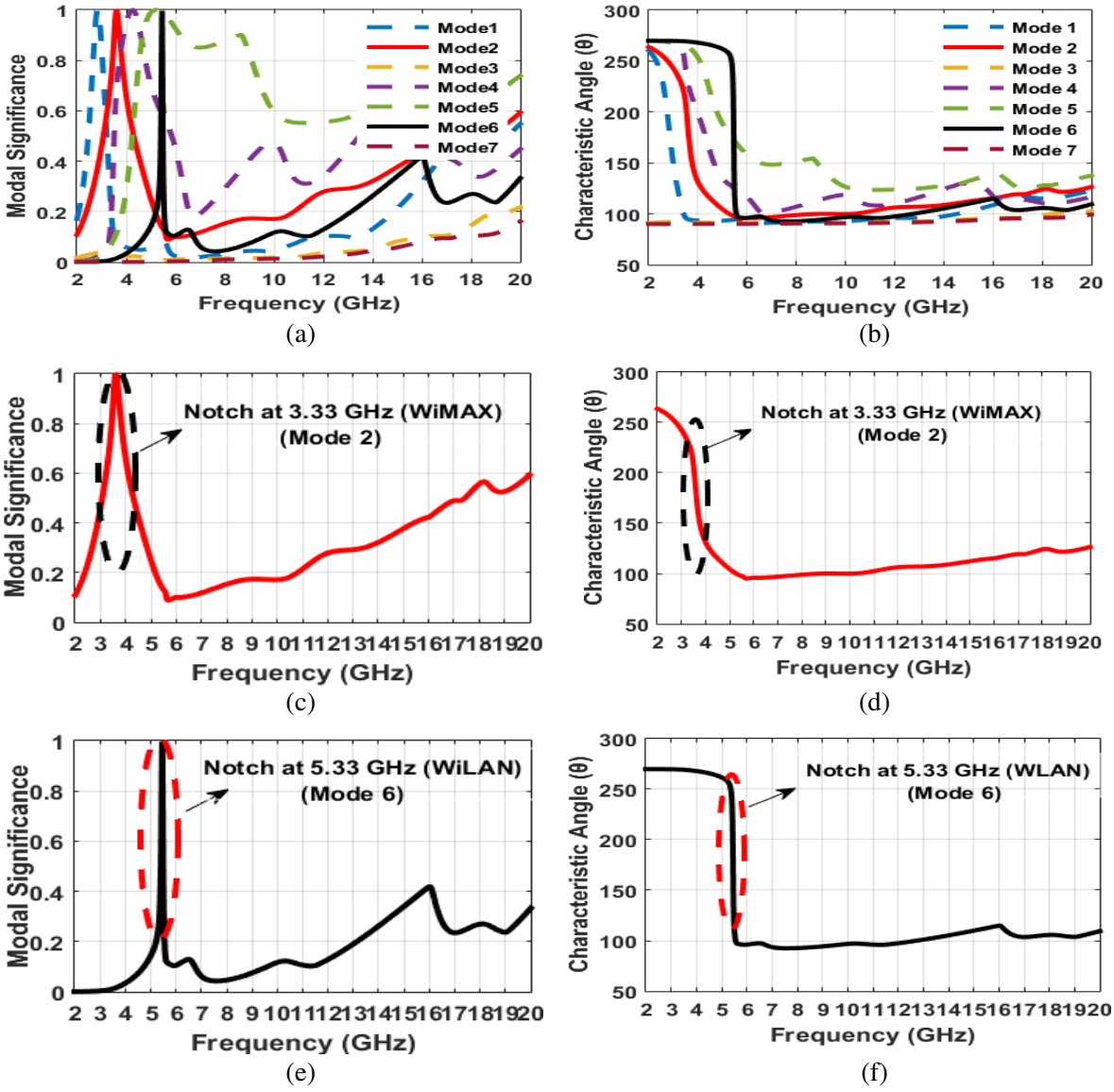

Figure 6. Proposed quadruple band notched EEP-UWB antenna with CMA analysis. (a) MS with 7 modes, (b) CA with 7 modes, (c) MS at WiMAX notched band, (d) CA at WiMAX notched band, (e) MS at WLAN notched band, (f) CA at WLAN notched band.

Figure 7(f) shows the current distributions to better comprehend the proposed dual notched bands. From Figure 7(f), at resonant frequencies of 2.88 GHz and 3.89 GHz, the surface currents are distributed uniformly over the entire surface of the proposed antenna structure represented by blue color scaling, and the surface currents at notch frequencies of 3.3 and 5.3 GHz are highly concentrated around the upper L-type stub and the L-type stubs etched on either side of the patch structure represented by red areas. Thus, the overall radiation is limited at 3.3 GHz and 5.3 GHz of frequencies which clearly indicates that the reported radiator effectively eliminates the interference due to WiMAX and WLAN bands, respectively.

The time domain performances of the proposed antenna in side-by-side and face-to-face arrangements are depicted in Figures 8(a) and (b). From Figure 8(c), the group delay of the proposed antenna varies in between 1.08 and 1.74 ns and 1.59 to 2.58 ns, except for the two notched bands WiMAX and WLAN, with fluctuating delays of 0.65 ns and 0.99 ns, for side-by-side and face-to-face configurations, respectively. From Figure 8(d), it is noticed that the isolation, S_{21} between the pair of

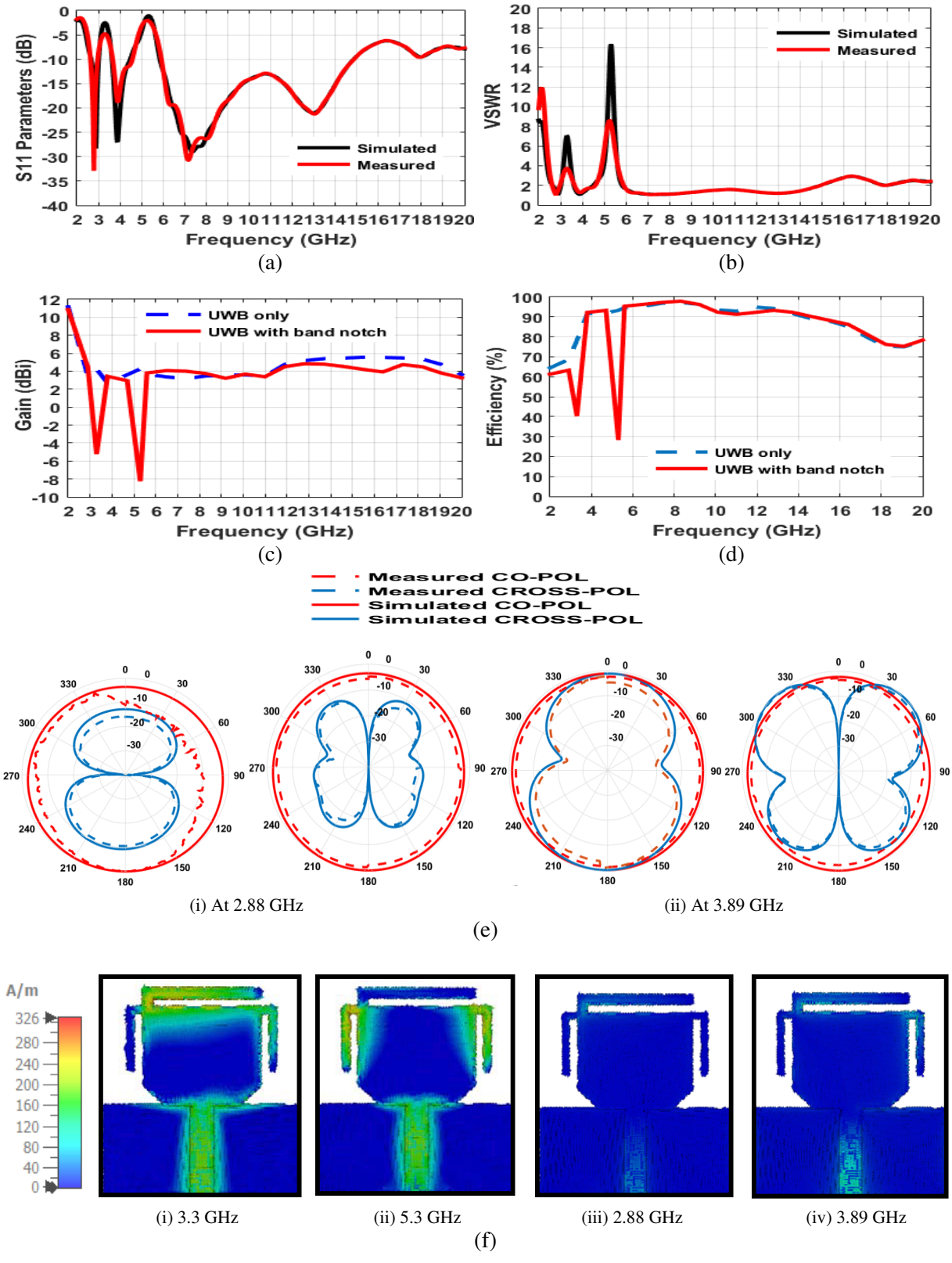

Figure 7. Frequency domain characteristics of proposed antenna. (a) S_{11} parameter, (b) VSWR, (c) peak gain, (d) radiation efficiency, (e) radiation patterns, (f) surface current distributions at notched frequencies, (i) 3.3 GHz, (ii) 5.33 GHz and resonant frequencies, (iii) 2.88 GHz, (iv) 3.89 GHz.

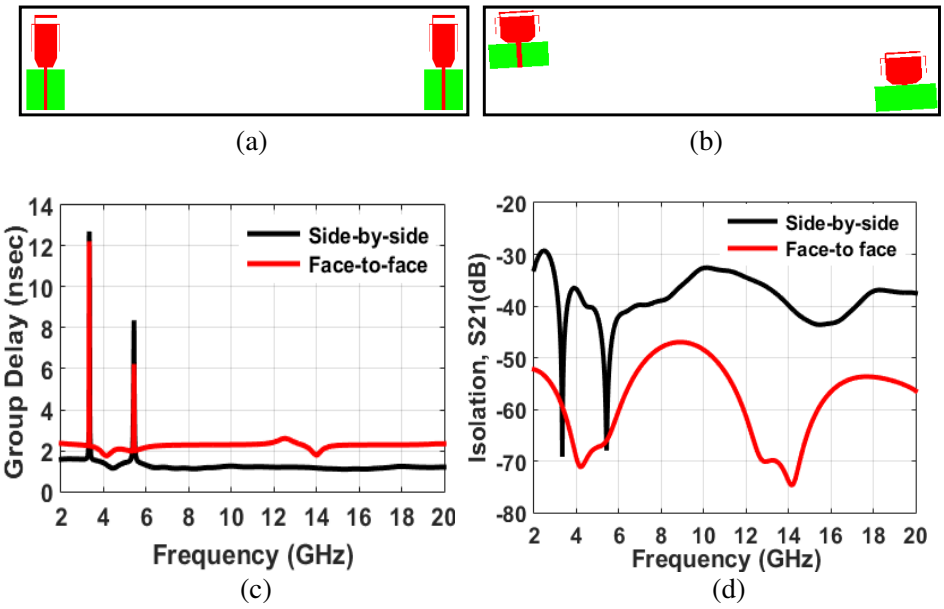

Figure 8. Time domain characteristics of proposed antenna. (a) Side-by-side, (b) face-to-face, (c) group delay, (d) isolation.

proposed antennas in side-by-side and face-to-face configurations, is noticed to be less than −30 dB over the entire operating bandwidth. The group delay fluctuations of less than 1 ns and a minimum isolation of $S_{21} < -30$ dB confirm a minimum pulse distortion of the proposed antenna [20].

The comparison of proposed radiator with literature antennas reported is illustrated in Table 2.

Table 2. Comparison among proposed and recent literature.

Ref.	Area (mm^2), λ_0	B.W, GHz	Notch Centre frequency, GHz	VSWR at notch frequency	Gain, (dBi)	Efficiency, %	CMA analysis for notched bands
[24]	$(0.31\lambda_0 \times 0.31\lambda_0)$	3.1–15	3.45, 5.6	4.5, 4	2.3–5	NR	NR
[25]	$(0.32\lambda_0 \times 0.30\lambda_0)$	2.7–10.6	4, 5.5	NR	2–5	NR	NR
[26]	$(0.29\lambda_0 \times 0.41\lambda_0)$	2.5–13	3.45, 5.3	NR	2.3–5.2	NR	NR
[27]	$(0.24\lambda_0 \times 0.24\lambda_0)$	1.8–10	2.4, 3.45	NR	1.6–4.6	NR	NR
[28]	$(0.41\lambda_0 \times 0.44\lambda_0)$	2.9–16	5.5, 7.5	5.9, 3.9	NR	NR	NR
[29]	$(0.40\lambda_0 \times 0.29\lambda_0)$	3.1–11.6	3.5, 5.5	NR	0.7–4.2	88	NR
[30]	$(0.30\lambda_0 \times 0.40\lambda_0)$	1.5–10.6	3.15, 5.34	6, 8, 5.9, 3.8	2.5–3.5	NR	NR
Prop	**$(0.25\lambda_0 \times 0.3\lambda_0)$**	**2.6–14.6**	**3.3, 5.33**	**7.02, 16.35**	**2.65–3.6 (stable)**	**97.85**	**performed**

λ_0 — Wavelength at lower frequency, B.W — Bandwidth, NR — Not Reported.

5. CONCLUSION

An ultra-wideband antenna with dual band notch characteristics checked by characteristic mode analysis (CMA) is reported. The proposed radiator consisting of a notched rectangular patch with a microstrip line feed and a rectangular DGS provides an impedance bandwidth of 2.6–14.6 GHz with a fractional bandwidth of 139%. The dual band notched characteristics are achieved by etching L-type stubs on top and both sides of patch structure to notch WiMAX and WLAN bands at centre frequencies of 3.3 GHz

and 5.33 GHz, respectively. The high VSWR values 7.02 and 16.35 of the proposed antenna confirm that the two notched bands effectively suppress the interference from WiMAX and WLAN. Furthermore, the dual notched bands performance of the proposed antenna is verified by using characteristic mode analysis (CMA) by analysing the modal significance and characteristic angle. Thus, the characteristics of proposed antenna having a peak efficiency of 97.85% at 8.3 GHz, a stable gain fluctuation of 2.65–3.6 GHz, and compact dimension of $0.25\lambda_0 \times 0.30\lambda_0$ make it suitable for portable UWB wireless applications.

REFERENCES

1. Federal Communications Commission: First Report and Order on Ultra-Wideband Technology, FCC 02-48, Washington, DC, 2002.
2. Devana, V. N. K. R. and A. M. Rao, "Dual band rejection UWB antenna using slot and a novel modified Ψ-shaped parasitic," *2020 7th International Conference on Smart Structures and Systems (ICSSS)*, 2020, doi: 10.1109/ICSSS49621.2020.9202357.
3. Sultan, K. S. and H. H. Abdullah, "Planar UWB MIMO-diversity antenna with dual notch characteristics," *Progress In Electromagnetics Research C*, Vol. 93, 119–129, 2019.
4. Devana, V. N. K. R. and A. M. Rao, "A compact 3.1–18.8 GHz triple band notched UWB antenna for mobile UWB applications," *IRO Journal on Sustainable Wireless Systems*, Vol. 2, No. 1, 265–276, 2020.
5. Garg, R. K., M. V. D. Nair, S. Singhal, and R. Tomar, "A miniaturized ultra-wideband antenna using "modified" rectangular patch with rejection in WiMAX and WLAN bands," *Microwave and Optical Technology Letters*, Vol. 63, No. 4, 1271–1277, 2020.
6. Medkour, H., M. Cheniti, A. Narbudowicz, S. Das, E. Vandelle, and T. P. Vuong, "Coplanar waveguide-based ultra-wide band antenna with switchable filtering of WiMAX 3.5 GHz and WLAN 5 GHz signals," *Microwave and Optical Technology Letters*, Vol. 62, No. 6, 2398–2404, 2020.
7. Devana, V. N. K. R. and A. M. Rao, "A novel dual band notched MIMO UWB antenna," *Progress In Electromagnetics Research Letters*, Vol. 93, 65–71, 2020.
8. Zou, Q. and S. Jiang, "A compact flexible fractal ultra-wideband antenna with band notch characteristic," *Microwave and Optical Technology Letters*, Vol. 63, No. 3, 895–901, 2021.
9. Devana, V. N. K. R. and A. M. Rao, "Design and parametric analysis of beveled UWB triple band rejection antenna," *Progress In Electromagnetics Research M*, Vol. 84, 95–106, 2019.
10. Orugu, R. and N. Moses, "Coplanar waveguide-based ultra-wide band antenna with switchable filtering of WiMAX 3.5 GHz and WLAN 5 GHz signals," *International Journal of Numerical Modelling: Electronic Networks, Devices and Fields*, Vol. 34, No. 1, e2806, 2021.
11. Devana, V. N. K. R. and A. M. Rao, "A novel fan shaped UWB antenna with band notch for WLAN using a simple parasitic slit," *International Journal of Electronics Letters*, Vol. 7, No. 3, 352–366, 2019.
12. Harrington, R. F. and J. R. Mautz, "Theory of characteristic modes for conducting bodies," *IEEE Transactions on Antennas and Propagation*, Vol. 19, No. 5, 622–628, 1971.
13. Chen, Y. and C.-F. Wang, "Electrically small UAV antenna design using characteristic modes," *IEEE Transactions on Antennas and Propagation*, Vol. 62, No. 2, 535–545, 2014.
14. Perli, B. R. and A. M. Rao, "Design of a wideband hexagonal monopole antenna with L-slot using characteristic mode analysis," *International Journal of Electronics*, Vol. 108, No. 8, 1340–1359, 2021.
15. Elias, B. B. Q., P. J. Soh, A. A. Al-Hadi, P. Akkaraekthalin, and G. A. E. Vandenbosch, "A review of antenna analysis using characteristic modes," *IEEE Access*, Vol. 9, 98833–98862, 2021.
16. Newton, M. E., K. Ma, Y. Luo, N. Yan, and B. Tang, "Dual-mode wideband slotted patch antenna using characteristic mode analysis and low-cost SISL technology," *Microwave and Optical Technology Letters*, Vol. 64, No. 3, 583–588, 2022.
17. Garbacz, R. J. and R. H. Turpin, "A generalized expansion for radiated and scattered fields," *IEEE Transactions on Antennas and Propagation*, Vol. AP-19, 348–358, May 1971.

18. Devana, V. N. K. R. and A. M. Rao, "Design and analysis of dual band notched UWB antenna using a slot in feed and asymmetrical parasitic," *IETE Journal of Research*, 2020, doi: 10.1080/03772063.2020.1816226.
19. Khandelwal, M. K., B. K. Kanaujia, and S. Kumar, "Defected ground structure: Fundamentals, analysis, and applications in modern wireless trends," *International Journal of Antennas and Propagation*, Vol. 2017, 2017.
20. Devana, V. N. K. R. and A. M. Rao, "Compact UWB monopole antenna with quadruple band notched characteristics," *International Journal of Electronics*, Vol. 107, No. 2, 175–196, 2020.
21. Devana, V. N. K. R. and A. M. Rao, "A compact fractal dual high frequency band notched UWB antenna with a novel SC-DGS," *Analog Integrated Circuits and Signal Processing*, Vol. 107, 145–153, 2021.
22. Devana, V. N. K. R. and A. M. Rao, "A compact flower slotted dual band notched ultrawideband antenna integrated with Ku band for ultrawideband, medical, direct broadcast service, and fixed satellite service applications," *Microwave and Optical Technology Letters*, Vol. 63, No. 2, 556–563, 2021.
23. Devana, V. N. K. R. and A. M. Rao, "A novel compact fractal UWB antenna with dual band notched characteristics," *Analog Integrated Circuits and Signal Processing*, Vol. 110, 349–360, 2022.
24. Sultan, K. S. and H. H. Abdullah, "Circular monopole ultra-wideband (UWB) antenna with reconfigurable band-notched characteristics," *2020 IEEE 23rd International Multitopic Conference (INMIC)*, 2020, doi: 10.1109/INMIC50486.2020.9318099.
25. Kadam, A. A. and A. A. Deshmukh, "Pentagonal shaped UWB antenna loaded with slot and EBG structure for dual band notched response," *Progress In Electromagnetics Research M*, Vol. 95, 165–176, 2020.
26. Li, J. and Y. Sun, "Design of reconfigurable monopole antenna with switchable dual band-notches for UWB applications," *Progress In Electromagnetics Research C*, Vol. 96, 97–107, 2019.
27. Chilukuri, S. and S. Gogikar, "A CPW-fed denim based wearable antenna with dual band-notched characteristics for UWB applications," *Progress In Electromagnetics Research C*, Vol. 94, 233–245, 2019.
28. Sanyal, R., S. Coomar, D. Chanda (Sarkar), P. S. Bera, and P. P. Sarkar, "Design of UWB monopole antenna with 5.5/7.5 GHz enhanced and controllable dual band rejection characteristics," *2020 IEEE International Conference for Convergence in Engineering*, 325–329, 2020, doi: 10.1109/ICCE50343.2020.9290693.
29. Mayuri, P., N. D. Rani, N. B. Subrahmanyam, and B. T. P. Madhav, "Design and analysis of a compact reconfigurable dual band notched UWB antenna," *Progress In Electromagnetics Research C*, Vol. 98, 141–153, 2020.
30. Kadam, A. A., A. A. Deshmukh, K. P. Ray, and S. B. Deshmukh, "Dual band-notched UWB antenna with L-shaped slots and triangular EBG structures," *2019 IEEE Indian Conference on Antennas and Propagation (InCAP)*, 2020, doi: 10.1109/InCAP47789.2019.9134452.